Exploring the Breast Cancer Inhibitor from Flavone Subclass: *In Silico* and *In Vitro* Assays

Dwi Syah Fitra Ramadhan[1*], Nurisyah Nurisyah[1], Asyhari Asyikin[1], Arfan Arfan[2], Loly Subhiaty Idrus[2], Hooi Chia Tang[3], Azlina Razak[4], and Hana Chen[5]**

[1]*Department of Pharmacy, Poltekkes Kemenkes Makassar, Jl. Baji Gau No. 10, Makassar 90222, Indonesia*

[2]*Faculty of Pharmacy, Universitas Halu Oleo, Jl. H.E.A. Mokodompit No. 1, Kendari 93232, Indonesia*

[3]*Department of Microbiology, Faculty of Medicine, Manipal University College Malaysia, Bukit Baru 75150, Melaka, Malaysia*

[4]*Department of Physiology, International Medical School, Management and Science University, Selangor 40100, Malaysia*

[5]*Department of Community Medicine, Faculty of Medicine, University of Cyberjaya, Cyberjaya 63000, Selangor, Malaysia*

*** Corresponding author:**

email: dwisyahfitra@poltekkes-mks.ac.id; nurisyah@poltekkes-mks.ac.id***

Received: November 4, 2025
Accepted: February 19, 2026

DOI: 10.22146/ijc.112819

Abstract: *Flavones, a subclass of flavonoids, are widely recognized for their diverse biological activities, including antioxidant, anti-inflammatory, and anticancer effects. Amentoflavone, a naturally occurring biflavonoid, has attracted attention for its potential to modulate cancer-related molecular targets. This study investigated the anticancer potential of amentoflavone against estrogen receptor alpha (ERα), a key therapeutic target in ER-positive breast cancer, using an integrated* in silico *and cytotoxicity approach. Molecular docking analysis using AutoDock4 demonstrated that amentoflavone binds strongly to ERα with a binding affinity of −37.03 kJ/mol and exhibits interaction similarity with the native ligand 4-hydroxytamoxifen (−48.27 kJ/mol). A 100-ns molecular dynamics simulation confirmed the stability of the amentoflavone–ERα complex, as indicated by stable RMSD, RMSF, SASA, and radius of gyration values, along with favorable MM/PBSA binding energy. Cytotoxicity evaluation using the MTT assay in T47D breast cancer cells showed that amentoflavone exhibited moderate cytotoxicity (IC_{50} = 169.547 ± 34.1651 μg/mL), supported by dose-dependent apoptotic morphological changes. These findings suggest that amentoflavone has potential as a natural lead compound for further optimization and development of ERα-targeted therapies in ER-positive breast cancer.*

Keywords: *breast cancer; flavone; estrogen receptor alpha; in silico; cytotoxicity assay*

■ INTRODUCTION

Breast cancer is one of the leading causes of cancer-related deaths among women worldwide [1]. According to Global Cancer Statistics (GLOBOCAN), the incidence of breast cancer continues to rise each year, including in Indonesia [2]. Although various therapies such as chemotherapy, targeted therapy, and immunotherapy have been developed, treatment effectiveness still faces major challenges, particularly due to toxic side effects, drug resistance, and high costs. Therefore, the search for natural compounds with strong anticancer potential and minimal side effects has become a major focus [3].

Estrogen receptor alpha (ERα) is a type of estrogen receptor that plays a crucial role in regulating gene expression and cellular behavior, particularly in estrogen-responsive tissues such as the breast [4]. ERα is a primary target in ER-positive breast cancer, where its presence serves as a biomarker for diagnosis and therapeutic selection [5]. The activity of ERα can be inhibited by antagonists that suppress cell proliferation and induce apoptosis in cancer cells [6]. ERα functions as both a cytoplasmic and a nuclear receptor that binds estrogen and subsequently translocates to the nucleus to modulate the transcription of target genes. The regulation of ERα can also be influenced by epigenetic

mechanisms, such as DNA methylation, which affects the expression of this receptor gene [4].

Flavones, a subclass of flavonoids, have been extensively studied for their broad biological activities, particularly as antioxidants, anti-inflammatories, and anticancer agents [7]. These compounds naturally occur in various plants, including several endemic species of Indonesia [8-9]. Previous study had demonstrated that flavones such as apigenin and luteolin can induce apoptosis, inhibit cancer cell proliferation, and suppress oncogenic signaling pathways, including ERα signaling, which play crucial roles in breast cancer development [10].

The *in silico* approach has emerged as an efficient and rapid method for predicting compound–protein interactions, evaluating pharmacokinetic and toxicity profiles, and screening potential candidate compounds prior to further *in vitro* or *in vivo* testing [11]. The combination of *in silico* modeling and cytotoxicity assays can provide more comprehensive insights into the identification of flavones from Indonesian isolates with potential as breast cancer therapeutic agents [12]. This study aims to explore the anticancer activity of flavone-class compounds from Indonesian isolates against breast cancer using *in silico* and cytotoxicity approaches. Specifically, it aims to analyze molecular interactions between flavone compounds and the ERα receptor using molecular docking and molecular dynamics (MD) simulations to evaluate binding potential and complex stability. Furthermore, this study will identify the cytotoxic effects of the best-performing flavone compounds identified by simulation on breast cancer cells using the MTT assay to determine IC_{50} values as indicators of cytotoxic activity.

■ EXPERIMENTAL SECTION

Materials

Amentoflavone was selected as the test compound in this study. The three-dimensional (3D) structure of amentoflavone was obtained from the PubChem database. The crystal structure of ERα was retrieved from the RCSB Protein Data Bank (PDB ID: 3ERT). The native ligand, 4-hydroxytamoxifen, was used for docking validation. The T47D human breast cancer cell line was used for cytotoxicity evaluation. Materials used in the cytotoxic assay included phosphate buffered saline (PBS), MTT reagent, sodium dodecyl sulfate (SDS), hydrochloric acid (HCl), and culture media. All databases and materials were used as obtained from their respective sources.

Instrumentation

Computational analyses were performed on a personal computer equipped with an Intel® Core™ i9-12500 CPU @8 GHz, 32 GB RAM, a 2 TB hard drive, and an 8 GB NVIDIA GeForce RTX 4060. The operating systems used were Windows 11 and Linux Ubuntu 16.04. The software employed in this study included Gaussian09 and GaussView 5.0.8 for ligand optimization, AutoDock4.2 with MGLTools1.5.6 for molecular docking, BIOVIA Discovery Studio Visualizer 2016 for interaction analysis, GROMACS 2025.1 for MD simulations, ACPYPE for ligand topology generation, VMD 1.9.2 for trajectory visualization, and MMPBSA.py for binding free energy calculations.

Procedure

Molecular docking analysis

The target ligands were obtained from the Markherb database, and their 3D structures were downloaded from PubChem and optimized using Gaussian with the AM1 basis set. Bound ligands, water molecules, and irrelevant chains were removed [13]. Molecular docking was performed using AutoDock4 with the Lamarckian Genetic Algorithm (population size of 100 individuals) [13-14]. Docking validation was carried out by redocking the native ligand (RMSD < 2 Å) prior to docking the isolated compounds. Binding affinity energies and amino acid interactions were analyzed according to validated methodologies [15].

MD simulation

MD simulations of the quercetin derivative–breast cancer receptor complexes were performed using GROMACS 2025.1 software [16]. Topology and ligand parameters were generated using the Antechamber Python Parser Interface (ACPYPE) tool [17]. The AMBER99SB-ILDN force field was applied to both ligands and proteins. Electrostatic interactions were

calculated using the Particle Mesh Ewald (PME) method [18]. The production simulations were conducted at constant temperature and pressure (310 K, 1 atm), with a 2 fs time step. All hydrogen bonds were constrained using the SHAKE algorithm, and a 100 ns trajectory was generated, saving coordinate frames every 20 ps. The MD simulation results were analyzed based on root mean square deviation (RMSD), root mean square fluctuation (RMSF), radius of gyration (Rg), solvent-accessible surface area (SASA), and molecular mechanics Poisson–Boltzmann surface area (MMPBSA) analyses [19].

Cytotoxic assay toward the T47D cell line

The compound with the best binding affinity was purchased from the Markherb herbal database (https://www.markherb.com/en/shop). A total of 1×10^4 MCF-7 cells per well were seeded into a 96-well plate and incubated for 24 h in a CO_2 incubator. The cells were then treated with each quercetin derivative at concentrations of 10, 50, 100, 200, 300, 400, and 500 µg/mL, followed by another 24-h incubation in a CO_2 incubator. After incubation, cell morphology was observed under a microscope. The medium was removed, and the wells were washed with PBS. Subsequently, 100 µL of MTT reagent (0.5 mg/mL) was added to each well, and the plate was incubated for 4 h in a CO_2 incubator. After the formation of visible formazan crystals, 100 µL of SDS in 0.01 M HCl was added as a stopping reagent. The plate was incubated overnight at room temperature in the dark, and the absorbance was measured at 570 nm using a microplate reader [20-21].

■ RESULTS AND DISCUSSION

Binding Energy Calculation

The docking analysis showed that all bioflavonoid ligands interact with the ERα receptor, with varying binding affinities, as summarized in Table 1. The obtained binding energy values ranged from −25.61 to −48.27 kJ/mol. The more negative the binding energy value, the stronger the interaction between the ligand and the receptor, indicating greater inhibitory potential toward ERα activity [15]. The native ligand, tamoxifen, showed the highest binding affinity value of −48.27 kJ/mol with an inhibition constant (Ki) of 3.46 nM. This value indicates that the native ligand interacts very strongly with the receptor's active site and thus serves as a reference for evaluating the potential of

Table 1. Binding affinity (ΔG) and inhibition constant (Ki) values of bioflavonoid ligands bound to ERα receptor

Ligand	ΔG (kJ/mol)	Ki (µM)
Native ligand 4-OHT	−48.27	3.46×10^{-3}
Tectochrysin	−29.45	6.87
Mosloflavone	−31.04	3.64
2,5-dihydroxy-7-methoxyflavanone	−33.72	1.24
Eupatorine	−28.41	10.56
Sinensetin	−27.52	14.97
Apiin	−25.61	32.77
Luteolin	−32.60	1.96
Chrysin	−31.21	3.43
Apigenin	−33.76	1.23
Amentoflavone	−37.03	0.33
Baicalein	−35.19	0.68
Nobiletin	−27.02	18.40
Tangeretin	−26.53	22.61
Baicalin	−30.58	4.41
Myricetin	−30.54	4.49
Vitexin	−30.12	5.29
Genkwanin	−30.00	5.55

the tested ligands. Although none of the tested compounds surpassed the native ligand in affinity, several compounds demonstrated comparable binding abilities. Among all ligands tested, amentoflavone ranked highest with a binding energy of −37.03 kJ/mol and a Ki of 326 nM, indicating a relatively strong interaction with ERα. Its biflavonoid structure allows multiple non-covalent interactions, including double hydrogen bonds, π–π stacking, and stable hydrophobic interactions, within the binding pocket. In addition to amentoflavone, compounds such as baicalein (−35.19 kJ/mol; 681.36 nM), apigenin (−33.76 kJ/mol; 1.23 μM), 2,5-dihydroxy-7-methoxyflavanone (−33.72 kJ/mol; 1.24 μM), and luteolin (−32.60 kJ/mol; 1.96 μM) also exhibited strong binding activity. The abundant hydroxyl groups in these compounds play an important role in forming hydrogen bonds with active residues at the ERα binding site.

Meanwhile, other ligands, such as chrysin, mosloflavone, genkwanin, vitexin, baicalin, and myricetin, showed binding energies ranging from –7.0 to –7.8 kJ/mol, with Ki values of 3–6 μM. These values indicate that the ligands still possess moderate inhibitory activity, though not as strong as those in the first group. Structures with more dominant methoxy substitutions generally exhibit reduced hydrogen-bonding capacity, thereby affecting the stability of the ligand–receptor complex. Some compounds, including sinensetin (−27.52 kJ/mol; 10.56 μM), nobiletin (−27.02 kJ/mol; 18.4 μM), and tangeretin (−26.53 kJ/mol; 22.61 μM), exhibited the lowest affinities toward the ERα receptor. The low binding energy values can be attributed to the predominance of nonpolar methoxy groups, which reduce the compounds' ability to form polar interactions with active residues in the binding pocket. The relationship between chemical structure and activity demonstrates that the greater the number of hydroxyl groups in a flavonoid structure, the stronger its ability to form hydrogen bonds that enhance receptor interaction [17]. Conversely, excessive methoxy substitution tends to decrease binding affinity.

Formed Amino Acid Interaction

The interaction analysis between the ligands and the ERα provides a deeper understanding of the binding mechanisms of flavone compounds at the receptor's active site. The results presented in Table 2 and Fig. 1 indicate that the tested ligands form several key interactions, similar to those observed for the native ligand 4-hydroxytamoxifen (4-OHT) (Fig. 1(a)), including hydrogen bonds and hydrophobic interactions, which are crucial for stabilizing the ligand–receptor complex [22].

The native ligand 4-OHT is known to interact with Glu353 and Arg394 through strong hydrogen bonds, as well as to form numerous hydrophobic interactions with residues such as Leu349, Leu384, Leu387, Met388, Leu391, Phe404, Gly420, Met421, Ile424, His524, and Leu525. These residues have been consistently reported as key components of the primary binding pocket in ERα, essential for both agonistic and antagonistic ligand activities. This interaction pattern serves as a reference for evaluating the similarity of the tested ligands' binding behavior.

Among all tested compounds, amentoflavone (Fig. 1(b)) exhibited the highest degree of similarity to the native ligand. Amentoflavone formed hydrogen bonds with Glu353, Gly420, and His524, showing a 50% similarity to the native ligand's hydrogen bonding pattern. This suggests that the hydroxyl groups in its biflavonoid structure can mimic the polar bonding pattern of 4-OHT. Furthermore, amentoflavone demonstrated 76.2% hydrophobic interaction similarity with the native ligand, particularly involving residues Leu349, Leu387, Leu391, Met388, Ile424, and Leu525. This high similarity indicates that amentoflavone likely occupies the same binding pocket as 4-OHT and may act as a competitive inhibitor of ERα.

Apigenin also exhibited 50% hydrogen bond similarity, forming bonds with Glu353, Gly521, and His524 (Fig. 1(c)), which are critical polar residues in the binding site. Its hydrophobic interaction similarity reached 52.4%, involving key residues such as Leu391, Met388, Leu428, and Phe404. These findings suggest that apigenin can form a stable complex, although one unfavorable interaction was observed with Leu525, likely due to suboptimal molecular orientation within the hydrophobic pocket. Meanwhile, baicalein demonstrated

Table 2. Comparison of hydrogen bonds, hydrophobic interactions, and unfavorable interactions between selected bioflavonoid ligands and the Erα receptor compared with the native ligand. The bolded residues indicating similar residues with native ligand

Receptor	Ligand	H-bond	Percentage of similar H-bonds with native ligand	Hydrophobic interaction	Percentage of similar hydrophobic interaction with the native ligand	Unfavorable	Percentage of similar unfavorable with native ligand
ERα (3ERT)	Native	Glu353, Arg394	-	Leu349, Leu387, Gly521, Leu391, His524, Gly420, Glu419, Met421, Ile424, Phe404, Met388, Leu525, Leu384, Met343, Leu428, Leu346, Ala350, Asp351, Trp383, Thr347, Leu354	-	-	-
	Amentoflavone	**Glu353**, **Gly420**, His524	**50%**	Leu539, **Leu354**, **Leu349**, **Leu387**, **Leu391**, **Met388**, **Leu428**, **Leu384**, Glu419, **Ile424**, **Met343**, **Gly521**, **Met421**, **Leu525**, **Leu346**, Thr345, **Ala350**, **Trp383**, **Asp351**, Leu536	**76.2%**	-	-
	Apigenin	Leu387, **Glu353**, Gly521, His524	**50%**	Arg394, **Ala350**, **Leu346**, **Phe404**, **Leu391**, **Leu428**, **Met388**, **Leu384**, Gly420, **Met343**, **Ile424**, **Met421**, **Leu349**	**52.4%**	Leu525	0%
	Baicalein	Glu353, **Arg394**, Leu387	**50%**	**Leu349**, **Ala350**, **Leu391**, **Met388**, **Leu346**, **Met421**, **Gly521**, **Leu525**, **His524**, **Ile424**, Gly420, Glu419, **Met343**, **Leu384**, Leu428	**57.1%**	-	-

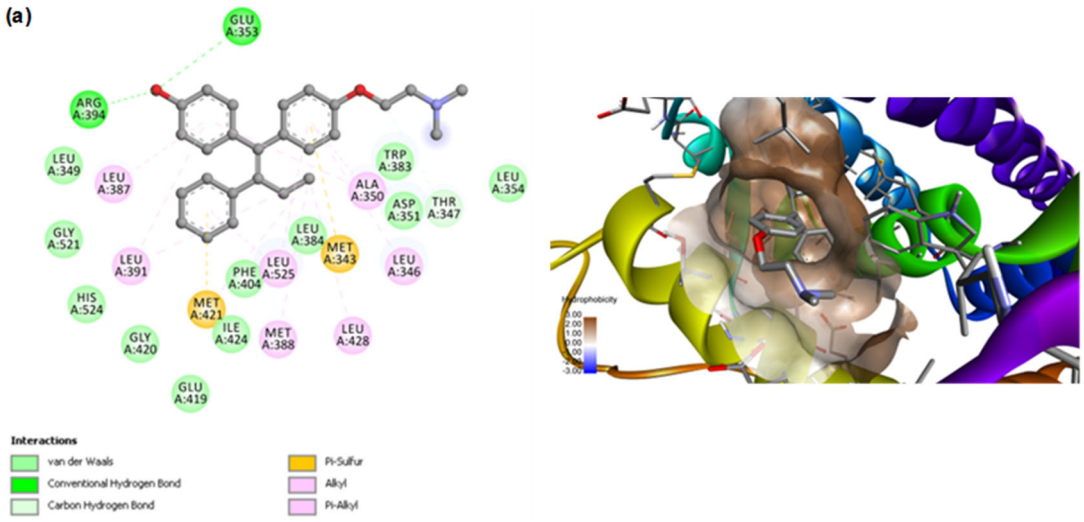

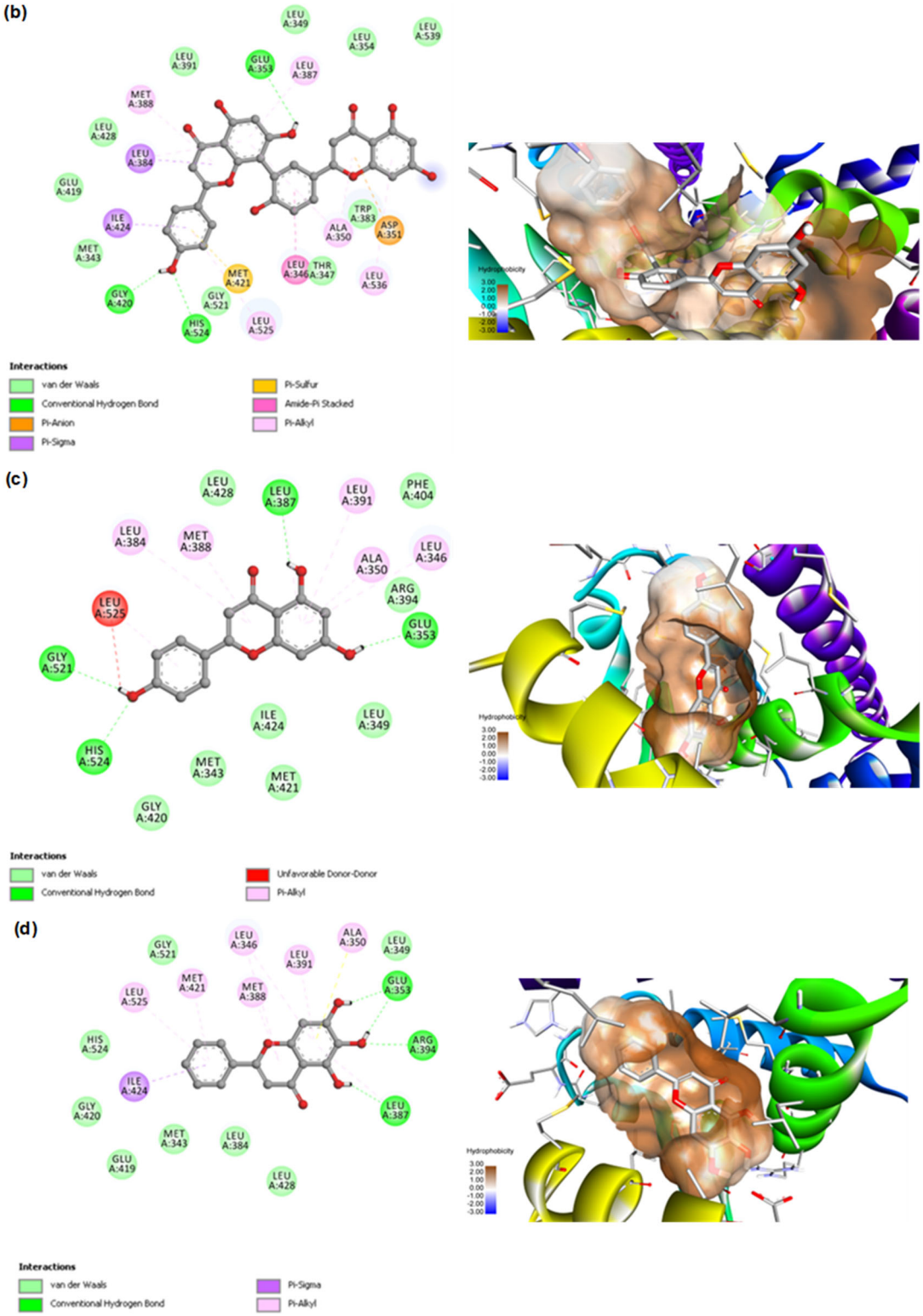

Fig 1. Visualization of amino acid residue interactions in the complexes of the (a) native ligand, (b) amentoflavone, (c) apigenin, and (d) baicalein with the ERα receptor

a binding pattern closely resembling that of the native ligand, with 50% hydrogen bond similarity through residues Glu353, Arg394, and Leu387 (Fig. 1(d)), and 57.1% hydrophobic interaction similarity. These residues are crucial for maintaining nonpolar interactions that help stabilize the ligand within the ERα binding pocket.

MD Simulation

An MD simulation was performed for 100 ns to evaluate the stability of the complexes formed between ERα and amentoflavone, compared with the native ligand 4-OHT. The analyzed parameters included RMSD, RMSF, SASA, and Rg, as shown in Fig. 2, as well as MMPBSA calculation [23]. The RMSD values (Fig. 2(a)) indicated the structural stability of the complexes throughout the simulation. The ERα–amentoflavone complex exhibited low and stable RMSD fluctuations around 0.25–0.35 Å, slightly lower than the native ligand (0.35–0.45 Å). This suggests that amentoflavone binding resulted in a relatively stable complex with minimal deviation from the initial conformation. RMSF values reflected the flexibility of each residue within the protein during the simulation (Fig. 2(b)). The fluctuation patterns of both complexes showed high similarity, with peak motions observed in the terminal loop regions (residues 240–260), which are typically flexible. No significant differences were found between the native ligand and amentoflavone, indicating that amentoflavone binding did not induce major changes in the local dynamics of the active residues of ERα. The SASA plot showed the protein's solvent-exposed surface area. The SASA value for the amentoflavone complex was slightly lower (approximately 130–145 nm^2) than that of the native ligand (140–155 nm^2), indicating a more compact and structurally stable complex (Fig. 2(c)). This decrease in SASA suggests that amentoflavone binding led to a minor compaction of the protein structure, potentially enhancing the interaction's stability. The Rg parameter measured the degree of protein compactness and density during the simulation. The Rg values for both complexes remained stable at 1.85–1.95 nm, with no significant fluctuations (Fig. 2(d)). The ERα–amentoflavone complex exhibited a slightly lower Rg value than the native ligand, suggesting a more compact structure and

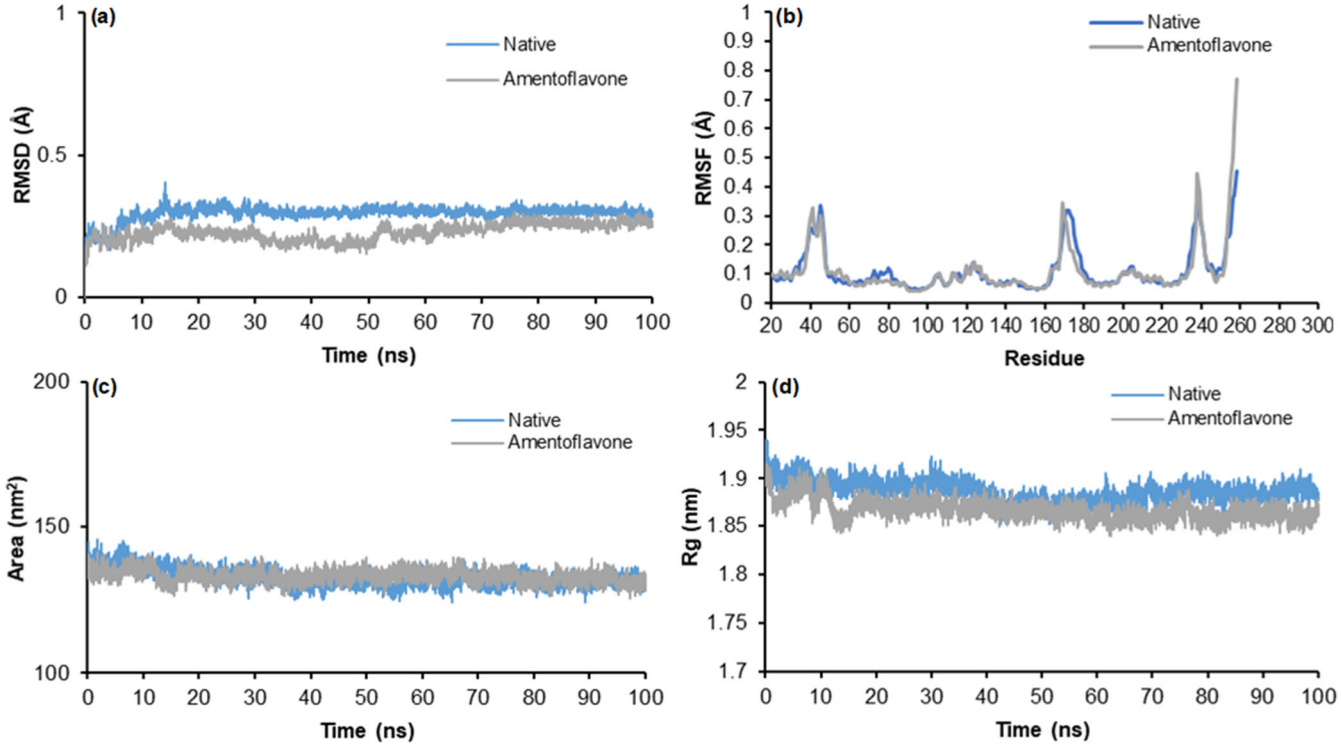

Fig 2. (a) RMSD, (b) RMSF, (c) SASA, and (d) Rg results from the MD simulation of ERα complexes with native ligand (4-OHT) and amentoflavone during a 100 ns trajectory

greater conformational stability throughout the simulation [24].

Subsequently, a quantitative analysis was performed using the MMPBSA method to re-evaluate the binding energy throughout the 100,000 ps simulation. The binding energy analysis using the MMPBSA approach provided an overview of the contribution of each energy component to the stability of the ERα ligand–receptor complex, as presented in Table 3. The analyzed parameters included van der Waals energy, electrostatic energy, polar solvation energy, SASA energy, and bond prediction energy [25-26]. The amentoflavone–ERα complex exhibited a lower van der Waals energy (−68.84 kJ/mol) compared to the native ligand (−51.04 kJ/mol), indicating stronger nonpolar interactions and dispersion forces between amentoflavone and the receptor's active site. These interactions significantly contribute to complex stability, as van der Waals forces are major components of ligand–receptor interactions involving the hydrophobic protein surface. Conversely, the electrostatic energy of amentoflavone (−7.34 kJ/mol) was much lower than that of the native ligand (−173.49 kJ/mol), suggesting that the binding of amentoflavone is predominantly driven by hydrophobic interactions rather than ionic or polar charge interactions. However, its solvation energy (30.07 kJ/mol) was also much lower than that of the native ligand (177.86 kJ/mol), indicating that the amentoflavone complex is more stable in an aqueous environment, requiring less solvation energy to maintain its conformation. In addition, the SASA energy for both ligands was relatively similar (around −7 kJ/mol), showing that the energetic contribution from solvent-exposed surfaces did not differ significantly. The bond prediction energy was also comparable between the two (approximately −54 kJ/mol), indicating that the main differences in complex stability arise from van der Waals and polar solvation energies. Overall, these results suggest that amentoflavone forms a complex with ERα that is comparable to the native ligand, with more dominant hydrophobic interactions and lower solvation energy than 4-OHT.

Cytotoxicity Assay of Amentoflavone Isolate

The amentoflavone isolate, identified as the compound with the best *in silico* simulation performance, was subsequently evaluated for its inhibitory activity against breast cancer cells using the MTT assay, and its IC_{50} value was determined. Fig. 3 presents the cytotoxicity results of the amentoflavone isolate against T47D breast cancer cells using the MTT method at seven concentration levels: 10, 50, 100, 200, 300, 400, and 500 µg/mL. The experiment was performed in triplicate (Rep1, Rep2, Rep3) to ensure data reproducibility. The results showed that cell viability decreased gradually with increasing amentoflavone concentration. At low concentrations (10 µg/mL), cell viability remained high, close to 100%, indicating that amentoflavone exerted minimal toxic effects on T47D cells at this dose. As the concentration increased to 100 µg/mL, cell viability decreased to approximately 70–80%, indicating the onset of proliferation inhibition. A more pronounced reduction was observed at 200–300 µg/mL, where cell viability

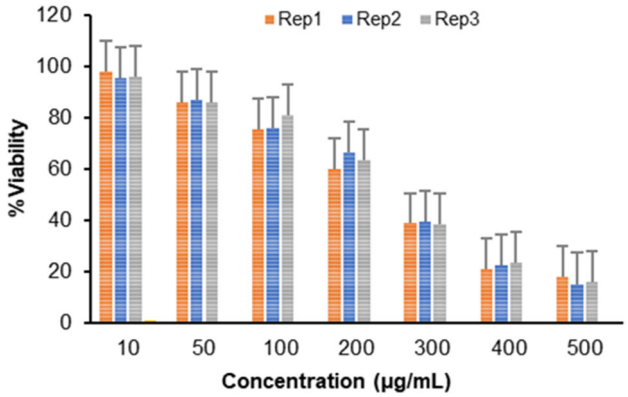

Fig 3. Percentage of cell viability at each concentration in three replications

Table 3. Binding energy calculations using the MMPBSA approach for a 100-ns simulation

Ligand	Van der Waals energy (kJ/mol)	Electrostatic energy (kJ/mol)	Polar solvation energy (kJ/mol)	SASA energy (kJ/mol)	Bond prediction energy (kJ/mol)
Native	−51.040	−173.490	177.860	−7.350	−54.030
Amentoflavone	−68.840	−7.340	30.070	−7.920	−54.020

dropped to 40–60%, suggesting a marked increase in cytotoxicity. At the highest concentrations (400–500 µg/mL), cell viability further decreased to 20–30%, indicating that most cells had undergone death or metabolic dysfunction due to amentoflavone exposure. Based on the dose–response curve, the IC_{50} value was estimated to be in the range of 200–250 µg/mL. From the calculated viability curve, the IC_{50} value obtained was 169.547 ± 34.1651 µg/mL, as detailed in Table 4. According to the toxicity classification, compounds with IC_{50} values between 201 and 500 µg/mL are categorized as weakly cytotoxic, whereas those with IC_{50} values below 200 µg/mL are classified as moderately cytotoxic [27]. Based on these results, amentoflavone's activity against T47D breast cancer cells falls within the moderate cytotoxicity range, indicating that the compound retains potential anticancer activity.

Further microscopic observations were performed to visualize morphological changes in ERα-positive breast cancer cells after treatment with varying concentrations of amentoflavone [28]. As shown in Fig. 4, the control group (Fig. 4(a)) displayed densely packed, polygonal cells firmly adhering to the culture surface, indicating healthy proliferation. At a low concentration of 10 µg/mL (Fig. 4(b)), mild morphological alterations emerged, including reduced cell density and early signs of cell rounding, suggesting mild cytotoxic stress. Increasing the concentration to 200 µg/mL (Fig. 4(c)) resulted in a marked reduction in cell density, accompanied by noticeable cell shrinkage and detachment—hallmarks of apoptosis induction. At the highest concentration (500 µg/mL; Fig. 4(d)), most cells lost adhesion and appeared rounded, indicating severe cytotoxicity and extensive cell death.

Correlation Between *In Silico* Binding Affinity and *In Vitro* Cytotoxic Activity

Although molecular docking and cytotoxicity assays represent different levels of biological complexity,

Table 4. IC_{50} value of amentoflavone obtained from MTT assay measurements

Replication	IC_{50} (µg/mL)	Average (µg/mL)	Standard deviation
1	202.477		
2	171.896	169.547	34.1651
3	134.268		

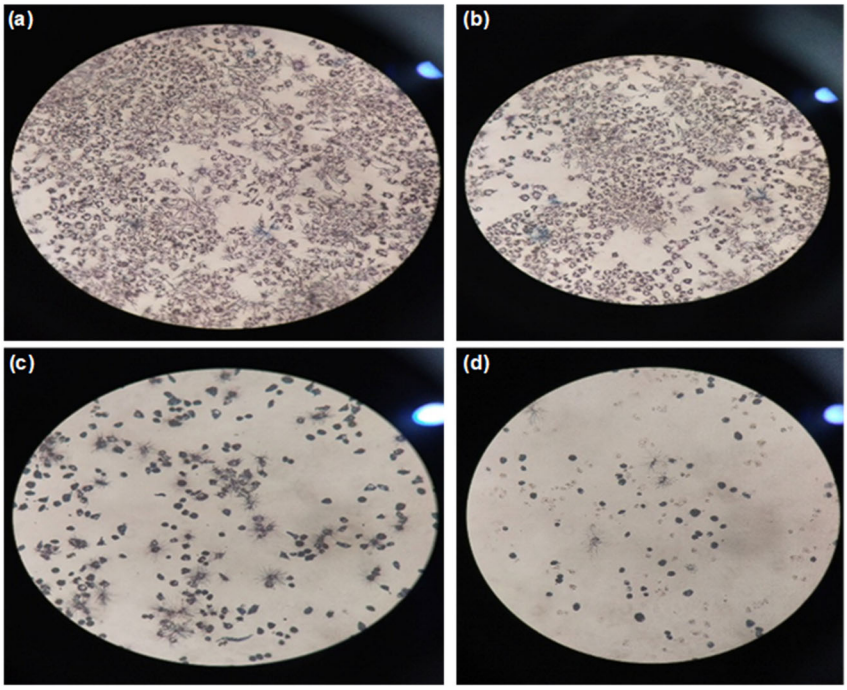

Fig 4. Microscopic observation of T47D cell death in the (a) control group and after treatment with amentoflavone at concentrations of (b) 10, (c) 200, and (d) 500 µg/mL

a qualitative relationship between *in silico* binding affinity and *in vitro* anticancer activity can be inferred in this study. Molecular docking results demonstrated that amentoflavone exhibited the most favorable binding affinity among the tested bioflavonoids (−37.03 kJ/mol), accompanied by strong interaction similarity with the native ligand 4-OHT at the ERα binding site. These findings suggest a high likelihood of effective receptor engagement, which may contribute to the observed biological activity.

This computational prediction was further supported by MD simulations, which confirmed the structural stability of the ERα–amentoflavone complex throughout the 100 ns trajectory. Stable RMSD, RMSF, SASA, and radius of gyration profiles, along with favorable MM/PBSA binding energy contributions—particularly dominant van der Waals interactions and lower polar solvation energy—indicate that amentoflavone forms a stable and energetically favorable complex with ERα. Such stability is a critical prerequisite for sustained receptor modulation under physiological conditions.

In the *in vitro* evaluation, amentoflavone demonstrated moderate cytotoxicity against ERα-positive T47D breast cancer cells, with a mean IC_{50} of 169.547 ± 34.1651 µg/mL. While the IC_{50} value does not correlate quantitatively with docking binding energies, the experimental results are consistent with the computational findings, indicating that compounds with stronger receptor binding and greater interaction stability tend to exhibit more pronounced antiproliferative effects. It is important to note that flavonoid-based compounds, such as amentoflavone, often exert anticancer effects through receptor modulation and signaling interference rather than direct cytotoxicity, which may explain the moderate IC_{50} value observed.

■ CONCLUSION

This study demonstrated that amentoflavone, a biflavonoid derived from Indonesian herbal isolates, shows promising anticancer potential against ERα-positive breast cancer. Molecular docking analysis revealed that amentoflavone binds strongly to the ERα with a binding affinity of −37.03 kJ/mol, showing interaction patterns comparable to the native ligand, 4-OHT. MD simulations over 100 ns confirmed the structural stability of the amentoflavone–ERα complex, supported by consistent RMSD, RMSF, SASA, Rg, and MMPBSA energy profiles. *In vitro* cytotoxicity testing using the MTT assay on T47D cells yielded an IC_{50} value of 169.547 ± 34.1651 µg/mL, classifying amentoflavone as a compound with moderate cytotoxic activity. Microscopic observation further supported these findings, showing dose-dependent morphological changes indicative of apoptosis. Overall, the integration of *in silico* and *in vitro* analyses confirms that amentoflavone has moderate cytotoxicity and a stable binding profile for ERα, suggesting it as a potential lead compound for the further development of natural product–based therapeutics targeting ERα-positive breast cancer.

■ ACKNOWLEDGMENTS

This research was funded by the Public Service Agency (BLU) of Poltekkes Kemenkes Makassar, Indonesia, under Research Grant No. DP.04.03/F.XII.12.3/4091/2025

■ CONFLICT OF INTEREST

The authors declare no conflict of interest.

■ AUTHOR CONTRIBUTIONS

Dwi Syah Fitra Ramadhan and Nurisyah conceptualized and designed the study, supervised the overall research process, and contributed to manuscript writing and revision. Asyhari Asyikin performed data curation, molecular docking, and assisted in the preparation of the manuscript. Arfan and Loly Subhiaty Idrus contributed to data analysis, validation of results, and interpretation of findings. Tang Hooi Chia and Azlina Abdul Razak provided methodological support, critical review, and academic input to improve the quality of the manuscript. Hana Chen contributed to data interpretation, language editing, and final proofreading of the manuscript. All authors read and agreed to the final version of this manuscript.

■ REFERENCES

[1] Madera, S., Izzo, F., Chervo, M.F., Dupont, A., Chiauzzi, V.A., Bruni, S., Petrillo, E., Merin, S.S., De Martino, M., Montero, D., Levit, C., Lebersztein, G., Anfuso, F., Roldán Deamicis, A., Mercogliano, M.F., Proietti, C.J., Schillaci, R., Elizalde, P.V., and Cordo Russo, R.I., 2022, Halting ErbB-2 isoforms retrograde transport to the nucleus as a new theragnostic approach for triple-negative breast cancer, *Cell Death Dis.*, 13 (5), 447.

[2] Bray, F., Laversanne, M., Sung, H., Ferlay, J., Siegel, R.L., Soerjomataram, I., and Jemal, A., 2024, Global cancer statistics 2022: GLOBOCAN estimates of incidence and mortality worldwide for 36 cancers in 185 countries, *Ca-Cancer J. Clin.*, 74 (3), 229–263.

[3] Nazarudin, M.F., Yasin, I.S.M., Mazli, N.A.I.N., Saadi, A.R., Azizee, M.H.S., Nooraini, M.A., Saad, N., Ferdous, U.T., and Fakhrulddin, I.M., 2022, Preliminary screening of antioxidant and cytotoxic potential of green seaweed, *Halimeda opuntia* (Linnaeus) Lamouroux, *Saudi J. Biol. Sci.*, 29 (4), 2698–2705.

[4] Hong, R., and Xu, B., 2022, Breast cancer: An up-to-date review and future perspectives, *Cancer Commun.*, 42 (10), 913–936.

[5] Jurzak, M., Ramos, P., Pilawa, B., and Bednarek, I.A., 2024, Comparative EPR studies on the influence of genistein on free radicals in non-irradiated and UV-irradiated MCF7, T47D and MDA-MB-231 breast cancer cells, *Biomedicines*, 12 (3), 518.

[6] Tahir, A., Plengsuriyakarn, T., Chittasupho, C., and Na-Bangchang, K., 2022, Potential of alpha-mangostin-loaded PLGA nanoparticles for cholangiocarcinoma treatment, *Polymers*, 14 (20), 4444.

[7] Pieracci, Y., Pistelli, L., Cecchi, M., Pistelli, L., and De Leo, M., 2022, Phytochemical characterization of *Citrus*-based products supporting their antioxidant effect and sensory quality, *Foods*, 11 (11), 1550.

[8] Wu, J., Zhou, T., Wang, Y., Jiang, Y., and Wang, Y., 2021, Mechanisms and advances in anti-ovarian cancer with natural plants component, *Molecules*, 26 (19), 5949.

[9] Yao, Z., Xu, X., and Huang, Y., 2021, Daidzin inhibits growth and induces apoptosis through the JAK2/STAT3 pathway in human cervical cancer HeLa cells, *Saudi J. Biol. Sci.*, 28 (12), 7077–7081.

[10] Khazeei Tabari, M.A., Iranpanah, A., Bahramsoltani, R., and Rahimi, R., 2021, Flavonoids as promising antiviral agents against SARS-CoV-2 infection: A mechanistic review, *Molecules*, 26 (13), 3900.

[11] Nivatya, H.K., Singh, A., Kumar, N., Sonam, S., Sharma, L., Singh, V., Mishra, R., Gaur, N., and Mishra, A.K., 2025, Assessing molecular docking tools: Understanding drug discovery and design, *Future J. Pharm. Sci.*, 11 (1), 111.

[12] Boulos, J.C., Chatterjee, M., Shan, L., and Efferth, T., 2023, *In silico*, *in vitro*, and *in vivo* investigations on adapalene as repurposed third-generation retinoid against multiple myeloma and leukemia, *Cancers*, 15 (16), 4136.

[13] Mariappan, A., Thanalakshmi, J., Sundar, S., Radha, S., Meenakumari, R., and Kaaruniya, G., 2023, *In silico* studies of active phytochemicals from Siddha medicinal herbs of Karisalai Chooranam against SARS-CoV-2 targets, *Res. J. Pharm. Technol.*, 16 (3), 1033–1040.

[14] Li, Y., and Singh, S.P., 2025, Computational screening of IL-1 and IL-6 inhibitors for rheumatoid arthritis: Insights from molecular docking and dynamics analysis, *Curr. Pharm. Des.*, 31 (27), 2200–2224.

[15] Chen, X., Yang, T., Huang, Y., Yang, Y., Li, X., Ma, Y., Long, H., Liao, D., Zhang, P., and Wen, W., 2026, Acacetin alleviates loperamide-induced functional constipation by inhibiting p53-mediated apoptosis in colonic epithelial cells, *Neurogastroenterol. Motil.*, 38 (4), e70298.

[16] Abraham, M.J., Murtola, T., Schulz, R., Páll, S., Smith, J.C., Hess, B., and Lindahl, E., 2015, GROMACS: High performance molecular simulations through multi-level parallelism from laptops to supercomputers, *SoftwareX*, 1-2, 19–25.

[17] Keser, M., Çamlı Pulat, Ç., Atmaca, H., Akgün, H., Albay, C., Menteşe, E., Bektaş, H., and Ilhan, S., 2026, Synthesis, characterization, and biological

evaluation of aliphatic-substituted benzimidazole derivatives: Induction of apoptosis, cell cycle arrest, and molecular docking in breast cancer cells, *Drug Dev. Res.*, 87 (2), e70267.

[18] Cui, J., Feng, Y., Yang, T., Wang, X., and Tang, H., 2023, Computer-aided designing peptide inhibitors of human hematopoietic prostaglandin D2 synthase combined molecular docking and molecular dynamics simulation, *Molecules*, 28 (15), 5933.

[19] Chikhale, R., Sinha, S.K., Wanjari, M., Gurav, N.S., Ayyanar, M., Prasad, S., Khanal, P., Dey, Y.N., Patil, R.B., and Gurav, S.S., 2021, Computational assessment of saikosaponins as adjuvant treatment for COVID-19: Molecular docking, dynamics, and network pharmacology analysis, *Mol. Diversity*, 25 (3), 1889–1904.

[20] Buranaamnuay, K., 2021, The MTT assay application to measure the viability of spermatozoa: a variety of assay protocols, *Open Vet. J.*, 11 (2), 251–269.

[21] Silchenko, A.S., Kalinovsky, A.I., Avilov, S.A., Popov, R.S., Dmitrenok, P.S., Chingizova, E.A., Menchinskaya, E.S., Panina, E.G., Stepanov, V.G., Kalinin, V.I., and Stonik, V.A., 2023, Djakonoviosides A, A_1, A_2, B_1–B_4 — Triterpene monosulfated tetra- and pentaosides from the sea cucumber *Cucumaria djakonovi*: The first finding of a hemiketal fragment in the aglycones; activity against human breast cancer cell lines, *Int. J. Mol. Sci.*, 24 (13), 11128.

[22] Wang, H., Yao, Q., Guo, Y., Zhang, Q., Wang, Z., Strasser, R.J., Valverde, B.E., Chen, S., Qiang, S., and Kalaji, H.M., 2022, Structure-based ligand design of tenuazonic acid derivatives with high herbicidal activity, *J. Adv. Res.*, 40, 29–44.

[23] Luo, L., Zhong, A., Wang, Q., and Zheng, T., 2022, Structure-based pharmacophore modeling, virtual screening, molecular docking, ADMET, and molecular dynamics (MD) simulation of potential inhibitors of PD-L1 from the library of marine natural products, *Mar. Drugs*, 20 (1), 29.

[24] Saini, R., Kumari, S., Bhatnagar, A., Singh, A., and Mishra, A., 2023, Discovery of the allosteric inhibitor from actinomyces metabolites to target $EGFR^{CSTMLR}$ mutant protein: Molecular modeling and free energy approach, *Sci. Rep.*, 13 (1), 8885.

[25] Askar, M., 2024, Computational quest to inhibit enoyl-acyl carrier protein reductase (InhA) enzyme in *Mycobacterium tuberculosis* from *Lannea coromandelica* (Houtt.) Merr. metabolite via molecular docking and dynamics, *Pharmacia*, 71, 1–10.

[26] Ren, J., Yuan, X., Li, J., Lin, S., Yang, B., Chen, C., Zhao, J., Zheng, W., Liao, H., Yang, Z., and Qu, Z., 2020, Assessing the performance of the g_mmpbsa tools to simulate the inhibition of oseltamivir to influenza virus neuraminidase by molecular mechanics Poisson–Boltzmann surface area methods, *J. Chin. Chem. Soc.*, 67 (1), 46–53.

[27] Widiandani, T., Tandian, T., Zufar, B.D., Suryadi, A., Purwanto, B.T., Hardjono, S., and Siswandono, S., 2023, *In vitro* cytotoxic activity of pinostrobin derivatives against T47D breast cancer cells, *J. Public Health Afr.*, 14 (1), 2516.

[28] Rezano, A., Ridhayanti, F., Rangkuti, A.R., Gunawan, T., Winarno, G.N.A., and Wijaya, I., 2021, Cytotoxicity of simvastatin in human breast cancer MCF-7 and MDA-MB-231 cell lines, *Asian Pac. J. Cancer Prev.*, 22 (1), 33–42.